PROCEEDINGS OF THE ROYAL SOCIETY A | MATHEMATICAL, PHYSICAL & ENGINEERING SCIENCES

The Artificial Radiation Belt Produced by the Starfish Nuclear Explosion

A. C. Durney, H. Elliot, R. J. Hynds and J. J. Quenby

Proc. R. Soc. Lond. A 1964 **281**, 565-583
doi: 10.1098/rspa.1964.0205

The artificial radiation belt produced by the Starfish nuclear explosion

By A. C. Durney, H. Elliot, R. J. Hynds and J. J. Quenby

Department of Physics, Imperial College of Science and Technology, Prince Consort Road, London, S.W. 7

Analysis of energetic particle flux measurements from Ariel I has led to a number of interesting conclusions about the effects of the Starfish nuclear explosion. It appears that the hydromagnetic shock wave generated by the explosion and propagated through the magnetosphere resulted in the disrupting of some outer belt electrons into the atmosphere. Following the explosion, a shell of electrons, centred at $L = 1{\cdot}12$ and continuously fed by fission fragments remaining in the vicinity of Johnston Island, was formed and lasted for at least 1 day. Arguments are given to support the view that the majority of the β-particles from the fission fragments were injected into the Earth's magnetic field at altitudes less than 1000 km, although some electrons—which probably came from the decay of neutral fission fragments—appeared as far out as $L = 6{\cdot}5$. At high L values the spectrum of the additional electrons was softer than that of the β-decay electrons from fission fragments.

1. Introduction

Many observations of the high-altitude nuclear test, Starfish, have now been reported in the scientific literature. The explosion occurred on 9 July 1962 at 09.00.09 u.t., 400 km above Johnston Island in the central Pacific Ocean. Satellites able to make energetic particle measurements on 9 July included Ariel I, Injun I, and Traac, while Telstar I was launched on the following day. Measurements at later times were made with instruments aboard Explorer XIV, Explorer XV, and various satellites launched by the United States Air Force. Early reports of the direct measurement of the newly created belt of artificial radiation by means of Injun I and Ariel I came from O'Brien, Laughlin & Van Allen (1962*a*) and from Durney, Elliot, Hynds & Quenby (1962). Observations of auroral displays, geomagnetic fluctuations and ionospheric disturbances which took place in the southern Pacific were summarized by J. B. Gregory in *Nature* (10 November 1962). Satellite measurements of the geographical distribution, energy spectrum and decay characteristics of the artificial belt of particles, together with observations on the synchrotron radiation from the electrons, were collected by Hess (1963*a*).

In this paper, concerned with the further analysis of the Ariel I data obtained after the Starfish explosion, three topics will be discussed. These are: the redistribution of electrons in the natural radiation belt by a hydromagnetic shock wave initiated by the explosion; the creation of a short-lived shell of electrons, continuously fed by fission fragments remaining over Johnston Island; and, finally, the appearance of energetic electrons at low altitudes on magnetic shells with high L values, these electrons having an energy spectrum softer than that due to β-particles produced by the decay of fission fragments. It is necessary to start with a brief description of the energetic particle detectors carried in Ariel I, which will be mentioned in this analysis. Other details are given in the preceding paper (Durney, Elliot, Hynds & Quenby 1964) and by Elliot, Quenby, Mayne & Durney (1961).

2. Energetic particle detectors in Ariel I

Ariel I was launched from Cape Canaveral on 26 April 1962 into an orbit of inclination 54°. On 9 July apogee occurred at 1209 km and perigee at 393 km. The satellite contained a heavily shielded Anton 302 counter and a Čerenkov detector with spherical geometry to detect heavy primary cosmic rays.

No experimental investigation of the Geiger-counter response to electrons has yet been attempted, but some estimates will be quoted.* In the direction where the amount of material is a minimum, the shielding consisted of 0·73 g/cm² Eccofoam, 1·13 g/cm² lead, 1·01 g/cm² aluminium, and 0·4 g/cm² iron. Electrons with energies of 7·4 and 10·5 MeV have, respectively, 10 and 50 % probabilities of penetrating this amount of material. For direct penetration by protons an energy of 50 ± 5 MeV is required. The counter will respond with a low efficiency to bremsstrahlung from electrons stopping in the shielding material. O'Brien, Van Allen, Laughlin & Frank (1962 *b*) have found this efficiency for an Anton 302, shielded by *ca.* 1 g/cm² magnesium and steel, to be *ca.* 10^{-5} at an energy of *ca.* 1 MeV. An approximate calculation yields an efficiency of *ca.* 10^{-6} at energies of *ca.* 0·5 MeV, and we regard the factor of 10^{-5} as an upper limit to the bremsstrahlung efficiency applicable here. The efficiency for γ-ray detection is about 0·4 % and the product of the omnidirectional geometrical factor and the fast charged particle efficiency is about 0·5 cm². For technical reasons, the counter circuitry was designed so that the apparent counting rate fell to zero at a true rate of 88 counts/s. All counting rates below 88/s quoted in this paper have been corrected for the onset of saturation.

The Čerenkov detector consisted of a hollow Perspex sphere, 10 cm in diameter and 3 mm thick, viewed by a 5 cm photomultiplier through a hole cut in the base of the sphere. At the time of Starfish, the circuitry was accepting pulses above two discriminator levels—one nominally equivalent to the light produced by relativistic heavy nuclei of $Z^2 = 36$ and the other of $Z^2 = 65$, Z being the nuclear charge in units of the charge on the electron. The counting rates above the two levels were monitored in sequence. Inner belt protons arriving within a very small solid angle could also cause pulses above the discriminator levels. This was due to the scintillation light produced by protons traversing the width of the glass face of the photomultiplier backing the photocathode. Calibration with a cyclotron beam revealed that the effect started for protons of 70 MeV while maximum pulse height was reached at 105 MeV. The response of the Čerenkov detector to cosmic rays was reduced to zero if the anode current of the photomultiplier exceeded the amount which the e.h.t. generator could supply. For example, a strong γ-ray source could cause this saturation effect, presumably as a result of Compton electrons generated in the optical media which produced sufficient light at the photocathode. We estimated that 2·4 MeV electrons had a 50 % probability of penetrating through the satellite skin and one thickness of the Čerenkov sphere, and that a flux of *ca.* 4×10^4 such electrons sterad^{-1} cm^{-2} s^{-1} could produce

* Note that our energy limits have been generally increased in these revised estimates, compared to those given by Durney *et al.* (1962).

sufficient Čerenkov light to cause saturation. The effects of electrons with lower energies are unknown, but it is likely that much higher fluxes would have been necessary to produce saturation.

Data on Starfish were obtained from 9 to 12 July, after which deterioration in the efficiency of the solar cells resulted in a serious loss of data. Up to 12 July, counting rates measured over $\frac{1}{2}$ min intervals were telemetered for over 80 % of the time in orbit. These counting rates have been organized in terms of $|B|$, the scalar magnitude of the Earth's magnetic field, and of L, the McIlwain (1961) parameter. For particles trapped in the Earth's magnetic field, the intensity along a line of force is a function of $|B|$ only. The L parameter is a function of the longitudinal adiabatic invariant and defines the magnetic shell on which the particles, mirroring at a given $|B|$, move as they drift around the earth. It is approximately constant along a line of magnetic force, and in a dipole field it is numerically equal to the distance in earth radii at which the line of force intersects the equatorial plane of the dipole. The B and L co-ordinates were computed by means of the program supplied by the Goddard Space Flight Center incorporating the Jensen and Cain 48-term expansion of the Earth's field for 1960.

3. The initial burst of particles

At the moment of the explosion, Ariel I was at an altitude of 815 km at latitude 52° S and longitude 163° E—a distance of 7400 km from Johnston Island. Ariel lay roughly on the same geomagnetic longitude as the point of the explosion but at a higher L value, namely, $L = 4{\cdot}76$ as opposed to $L = 1{\cdot}12$.

Table 1

time at middle of interval (U.T.) 9 July	Geiger-counter rate	Čerenkov-counter rate	Čerenkov-attenuator level
08.58.55·9	64	4	high
08.59.26·7	80	4	
08.59.57·4	72	8	
09.00.28·1	40	4	
09.00.58·8	0	8	
09.01.29·5	0	8	

Since the timing at the beginning of the event is important for some of our arguments later, we reproduce in table 1 the counting rates of the two detectors, together with the time at the middle of the sampling interval. The sampling period is 30·72 s but, because of the dead time associated with the encoder gate, the counts are in fact for a period of 26·9 s in the case of the Geiger counter and 28·8 s in the case of the Čerenkov detector.

These counting rates are plotted in figure 105, the moment of the explosion (09.00.09 U.T.) being taken as the zero of the time scale. During the sampling interval centred on 09.00.28 U.T. and including the instant of the explosion, the Geiger-counter rate dropped to 40 from an average value of 75 just before the explosion, while in the next interval saturation had occurred. The simplest

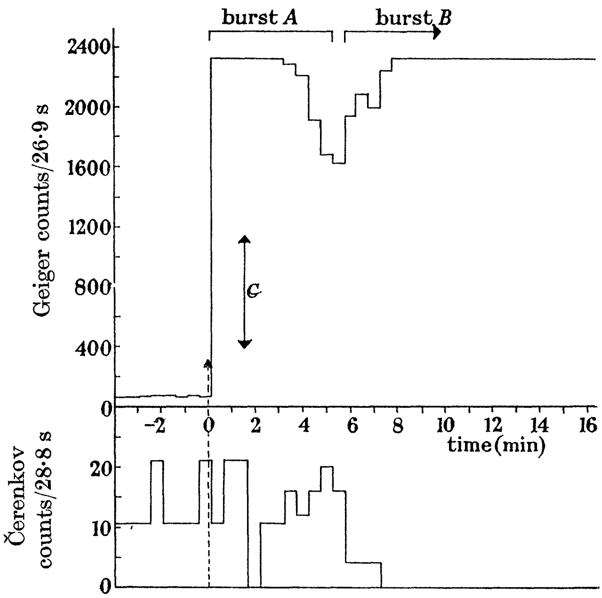

FIGURE 105. The Geiger-counter and Čerenkov-detector counting rates plotted as a function of time with the moment of the explosion taken as the zero of time. During burst *A*, only the Geiger counter saturates, while during burst *B* both detectors saturate. Arrow *C* corresponds to Ariel I passing through the Johnston Island magnetic meridian.

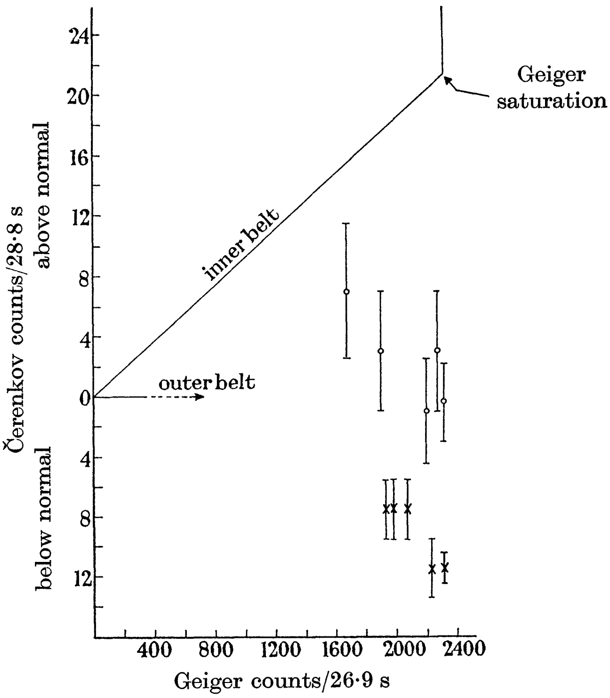

FIGURE 106. The departure of the Čerenkov-detector counting rate from the normal cosmic ray rate plotted against the Geiger-counter rate for naturally trapped inner and outer belt particles. Points are also shown from burst *A* (○) and burst *B* (×), the latter being typical of the response of the detectors to electrons from fission fragment decay.

interpretation of these numbers is that the Geiger counter responded to natural radiation for 40/75 of the 30·72 s interval and then saturated almost instantaneously due to the effects of Starfish. In this way a delay of 20 ± 5 s from the explosion time is obtained before the counter records an increase. Two bursts of radiation are distinguishable in figure 105: burst A, lasting about 6 min and showing on the Geiger counter only, and burst B, starting 6 min after the explosion, in which both detectors saturate.

An examination of the relative response of the two detectors during burst A yields some information on the type of particles causing the increase. Figure 106 shows the departure of the Čerenkov rate from the normal cosmic ray rate plotted against the Geiger rate for three different types of radiation. For protons in the inner belt, both detectors increase until the Geiger saturates, while for the outer belt electrons only the Geiger counter shows any increase, the Čerenkov showing no response at all. The points for burst B are typical of the response to electrons from fission fragments released in Starfish. Here the Čerenkov rate is reduced towards zero as the Geiger rate increases because of the high current drain in the photomultiplier. The points for burst A lie close to the line applicable to outer belt particles and do not seem to be attributable to the energetic fission fragment β-particles.

Three possible explanations for the particles in burst A have to be considered:

(*a*) They are directly observed γ-rays from the nuclear explosion.

(*b*) They are electrons resulting from neutron decay.

(*c*) They are outer belt electrons whose mirror point distribution is perturbed by a hydromagnetic disturbance resulting from the explosion.

We will discuss these possibilities in turn.

(*a*) *γ-ray origin for burst* A

It is conceivable that, following the explosion, plasma carrying fission fragments travelled along the line of force through the explosion point towards the equator, or that a plasma bubble was expelled from the Earth in a vertical direction due to the gradient in the magnetic pressure. Thus, although the explosion occurred below the optical horizon of Ariel I, the plasma with its associated γ-emission may subsequently have appeared above the horizon.

The emission of delayed γ-rays can be computed from the following formula:

$$F = [Y/r^2 t^{1\cdot 2}] \times 10^{12} \quad \text{(Latter, Herbst \& Watson 1961)},$$

where F is the γ-ray flux in quanta cm^{-2} s^{-1}, Y is the explosion yield in kilotons, t is the time in seconds, and r is the distance from the explosion in kilometres. In order to explain the onset of saturation in the Geiger counter after 20 s, we would require approximately one-tenth of the bubble to appear over the horizon, having propagated with a speed of 100 km/s; while to explain the continued saturation for a period of 200 s it is necessary for at least half the bubble to be above the horizon, having moved at a speed of 10 km/s. Neither of these possibilities seems likely.

An independent observation of a burst of radiation at this time has been reported by Edwards, Fenton, Fenton & Greenhill (1962). They recorded an increase in the counting rate of a Geiger counter carried in a balloon at an atmospheric depth of 80 g/cm^2 above Hobart, Tasmania. In view of the different optical horizons for Ariel I and the balloon, the 20 ± 5 s delay observed by Ariel I would correspond to a delay of 60 ± 15 s at the balloon, if we assume a constant velocity for the rise of the bubble. The Tasmanian results actually show a delay of 15 ± 7 s, which is therefore inconsistent with any reasonable motion of the plasma.

(b) *Neutron decay origin for burst* A

A fission explosion results in the production of neutrons with an average energy of 2 MeV, and the fraction of these which decays within the region of the Earth's magnetic field will supply some additional flux of trapped electrons. Assuming a yield of *ca.* 10^{26} neutrons from a 1-megaton explosion, we estimate very roughly the initial flux of electrons arriving at Ariel I from the neutron decay to have been *ca.* 10^5 cm^{-1} s^{-1}. Killeen, Hess & Lingenfelter (1963) calculate the flux close to the Earth of electrons that remained on the $L = 4$ shell to have been 10^5 cm^{-2} s^{-1} also. They have taken into account the decay both of fast neutrons and of albedo neutrons which were slowed down by the atmosphere and then scattered out into space again. If, on the other hand, we assume the Starfish explosion was entirely fusion in character, the neutron flux may have been increased by a factor of 20 (J. F. Kenney 1963, private communication). Thus, under the most extreme assumptions and using a counter efficiency of *ca.* 10^{-5} for the detection of *ca.* 0·5 MeV electrons, the maximum counting rate of the Geiger counter from neutron decays was 10/s. This is insufficient to have caused the observed saturation.

A further argument against a neutron decay origin for the initial burst lies in the time delay between the explosion and the observed increase. Since the velocity of the neutrons is *ca.* 2×10^9 cm/s, decay electrons would be expected to have arrived at Ariel I within 1 s of the explosion, while in fact the burst occurred with a delay of 20 s.

(c) *The redistribution of outer belt particles as an explanation of burst* A

An attractive explanation of burst *A* is that it represented a redistribution of natural particles in the outer belt. Such a redistribution could have been caused by a hydromagnetic shock initiated in the magnetosphere by the explosion and causing a breakdown of the Alfvén adiabatic invariant of motion for the trapped particles. This would have led to a redistribution of the particle mirror points and to the loss of some particles into the atmosphere. Using the Alfvén speed quoted by Parker (1961) as a function of distance from the Earth to represent the shock wave velocity, we find the travel time for the magnetic disturbances to have reached any point on the line of force through Ariel I at $L = 4·76$ to lie in the range 15 to 25 s. This is consistent with the observed delay.

It has already been shown that the ratio of the increase in Geiger-counter rate to that of the Čerenkov detector during burst *A* is compatible with the presence of particles having an energy spectrum similar to the spectrum of outer belt electrons. In order to estimate whether the total flux of outer belt electrons was sufficient to cause the observed increase after redistribution, we take the most favourable case and assume that the pitch angle distribution of the particles in the heart of the outer belt in the equatorial plane was made isotropic for the duration of the magnetic disturbance as a result of magnetic scattering by the field fluctuations. Then by Liouville's theorem the directional flux at Ariel I following the redistribution of particles was equal to the directional flux in the heart of the outer belt. Thus since Ariel I was close to the Earth, it measured a total particle flux of the order of half the omnidirectional flux in the maximum of the outer belt. Observations over several years by Van Allen and co-workers show that counting rates of between 10^4 and 10^5/s are obtained with Anton 302 counters shielded by *ca.* 1 g/cm^2 of material, in the heart of the outer belt. The Anton 302 counter in Ariel I was more heavily shielded than those flown by Van Allen, but in order to get a crude idea of the ratio of the response of the two counters we can compare the Ariel I counting rate and the counting rate of the 302 in Explorer IV during August 1958 (Van Allen, McIlwain & Ludwig 1959) at a similar geomagnetic position in the horn of the outer belt. Clearly the ratio of 1:20 obtained is rendered uncertain by the presence of intervening time variations, but using this estimate we expect a counting rate of between 200 and 2000/s at Ariel I during the initial burst as a result of appreciable magnetic scattering. The lower of these two counting rates is quite sufficient to have caused the observed saturation of the Geiger counter.

Reasonable criteria for a magnetic disturbance which will reduce the pitch angle distribution of trapped particles to an isotropic distribution are the presence of field changes comparable in magnitude to the size of the original static field, together with a scale-size of the disturbance equal to or smaller than the Larmor radii of the particles. The field strength in the equatorial plane on the $L = 4{\cdot}76$ shell is 290γ. Magnetic field changes of the order of 100γ were observed at Campbell Island ($L \sim 4$) south of New Zealand 2 min after the explosion (Gill 1962). However, the actual magnitude of the field fluctuations far out along this field line is not known: the sea-level observations, for example, may be distorted by the effects of particles precipitated into the ionosphere. The simple theory for a strong collisionless shock (see, for example, Gardner, Goertzel, Grad, Morawetz, Rose & Rubis 1958) suggests that the dimension of the front is *ca.* 1/40 of the ion Larmor radius, the ions having the Alfvén speed. This yields a scale size of *ca.* 0·3 km for the hydromagnetic disturbance at $L = 4{\cdot}76$—sufficient to scatter electrons with energies greater than 1 keV—whereas the bremsstrahlung response of the Geiger counter arises almost entirely from electrons of energy greater than 100 keV.

It is, of course, necessary that the energy present in the shock front should have been less than the total energy released by the nuclear explosion. Reliable estimates of the thickness of the shock are difficult to make, but a reasonable value, which should not yield an underestimate of the energy, is several times the ion Larmor radius, i.e. *ca.* 50 km at $L = 4{\cdot}76$. Using an energy density of $(\Delta H)^2/8\pi$ erg/cm^3 we find the energy contained in a shell of radius $L = 4{\cdot}76$ and width 50 km to be 2×10^{20} erg where we have put $\Delta H = 290\gamma$. The energy released in a 20-megaton fission explosion is $8 \cdot 4 \times 10^{23}$ ergs (*Nuclear explosions* 1956). Thus the total energy of 6×10^{22} ergs released by Starfish was at least 100 times the energy necessary for the shock wave.

To summarize, neutron decay electrons and γ-rays appear to be excluded as an explanation of the initial burst of particles, whereas a hydromagnetic shock does provide a plausible mechanism for the increased intensity. The increase started with a delay time which is consistent with the Alfvén speed, and estimates of the magnitude and scale of the shock indicate that appreciable disturbance of the pitch angles of particles in the equatorial plane at $L = 4 \cdot 76$ could have been produced. The flux of particles normally present in the outer belt is sufficient to have given the observed increase of particle flux in burst A, and the energy spectra of the particles in the burst appears to be similar to that for natural radiation belt electrons.

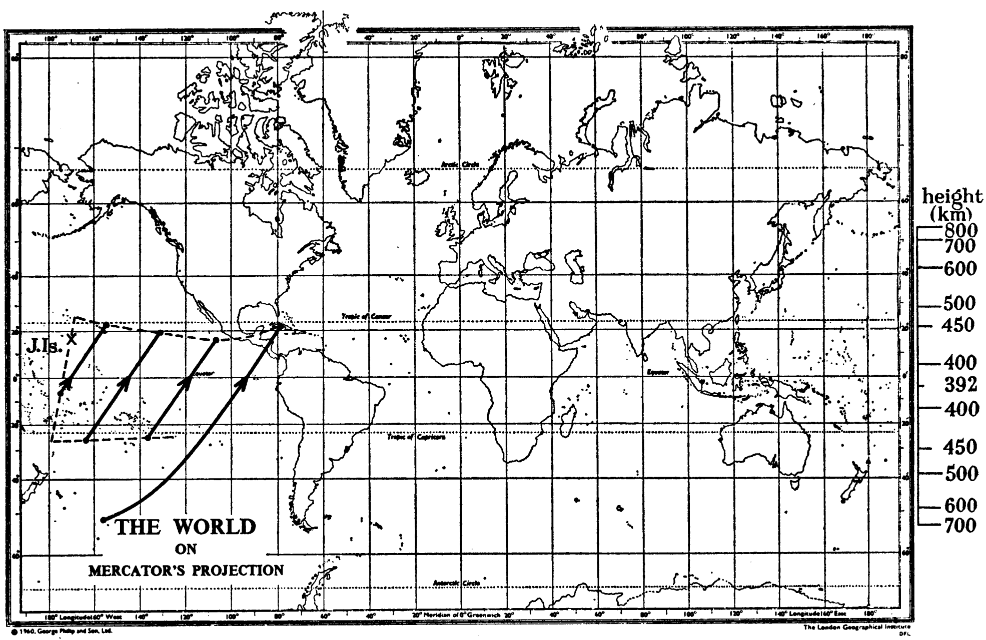

FIGURE 107. Positions of the subsatellite point where the Čerenkov detector saturated on the perigee portions of the orbits on 9 July.

4. The Johnston Island shell

Each Project Argus event caused a belt of radiation to form on the magnetic shell containing the point of the explosion. Similarly, following the Starfish explosion, Ariel I and Traac located an intense belt of radiation on the $L = 1 \cdot 12$ shell which passes 400 km above Johnston Island (Durney *et al.* 1962; Pieper 1963). This belt is illustrated in figure 107, which shows the subsatellite points where the Ariel Čerenkov detector saturated on the perigee portions of the orbit on 9 July. The corresponding Geiger counter rate was > 30 counts/s. Clearly, the particles in this belt are β-decay electrons from fission fragments, and since 10 % of these electrons have energies in excess of 2·7 MeV the Čerenkov detector is probably saturated as a result of the light produced by these electrons penetrating to the Perspex sphere.

Because of the westward motion of the satellite relative to the Earth, we were unable to observe the eastern extent of the Johnston Island shell until 10 July, when the intensity was very much reduced. However, it is known that the $L = 1{\cdot}1$ shell reaches the Earth in South America and the lifetime of the electrons drifting

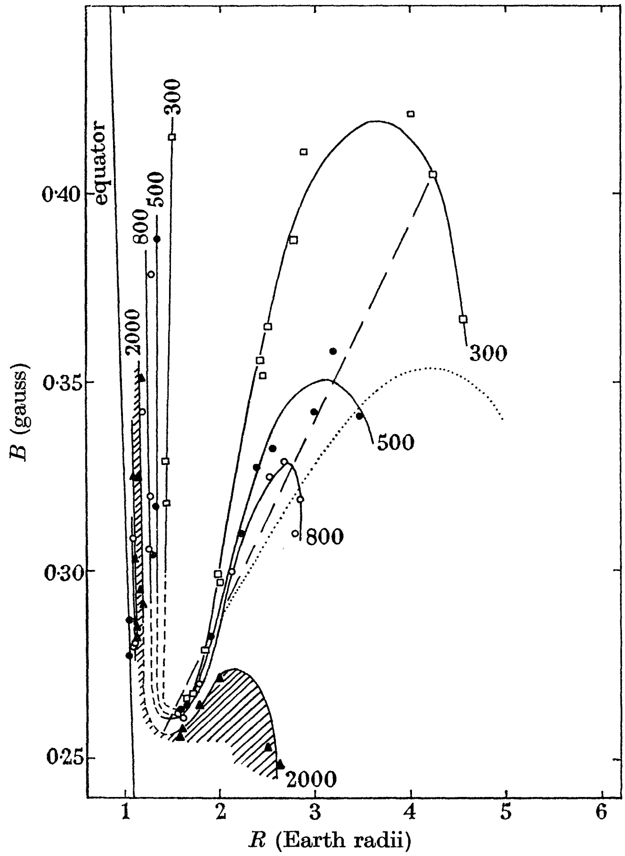

FIGURE 108. *B–L* plot of the excess of the Geiger-counter rate over the pre-Starfish measurements in the region east of Johnston Island and west of the South Atlantic anomaly. The numbers indicate counts per 26·9 s. The dashed line gives the lowest value of *B* found anywhere at sea level on the corresponding *L* shell, and the dotted line is the 300 counts 26·9 s contour derived from figure 110. Shaded regions correspond to Geiger-counter saturation.

eastward on the shell is only a few minutes. The shell must, therefore, be continuously fed by the decay of fission fragments remaining over Johnston Island. The fission fragments could be charged, in which case they could be trapped in the Earth's field, or they could be neutral, in which case they would need to have a slow rate of diffusion in the upper atmosphere. The sharp edge to the contours in figure 107, occurring just to the west of Johnston Island, is to be expected if the fragments are charged because of the slow westward drift of heavy ions. Pieper (1963) discusses these points more fully.

The excess of the Geiger-counter rate over pre-Starfish measurements in the region of this electron shell between Johnston Island and the South Atlantic anomaly is plotted for 9 July in figure 108, where the co-ordinates are $|B|$ and L for the point of observation. To present a more physical picture of the distribution of particles, we re-plot in figure 109 the intensity contours inferred from the individual points in figure 108, using an idealized dipole representation of the Earth's field to transform from (B, L) co-ordinates to (R, λ) co-ordinates (McIlwain 1961). R is the radial distance from the dipole and λ is the invariant magnetic

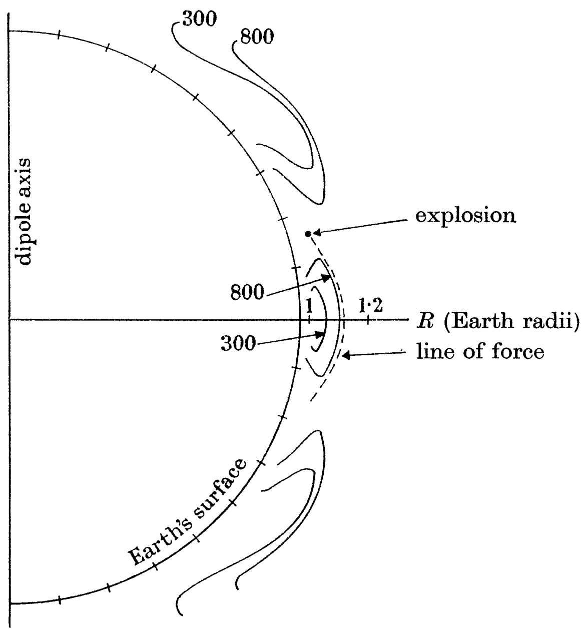

FIGURE 109. R–λ plot of the Geiger-counter intensity contours (counts per 26·9 s) inferred from figure 108 for a dipole representation of the Earth's field. The Earth's surface is shown as it occurs relative to the L shells in the meridian of Johnston Island.

latitude. We also show in figure 109 the position of the Earth's surface as it occurs relative to the L shells in the meridian through Johnston Island. At other longitudes, where for example the $L = 1{\cdot}12$ shell disappears below the Earth's surface, the lower contours would lie below the Earth's surface.

Returning to figure 108, the Johnston Island shell appears as a narrow belt of radiation with peak intensity lying between $L = 1{\cdot}12$ and $L = 1{\cdot}18$. Traac observed this shell at about the same L value but at a higher altitude corresponding to $B \sim 0{\cdot}24$ G. From the range of L values containing the peak intensity in the shell we can estimate the height of the particle source above Johnston Island. The magnetic shells $L = 1{\cdot}12$ and $L = 1{\cdot}18$ pass above Johnston Island at altitudes of 400 and 700 km, respectively. It appears likely, therefore, that the main bulk of fission fragment debris from the explosion reached an altitude of no more than 700 km. There would therefore seem to be no evidence for the supposition that the plasma bubble was diamagnetically expelled to a distance of several Earth radii.

In addition to this well-defined shell, figure 108 shows the presence of a broad belt of particles existing between $L = 2{\cdot}5$ and $L = 4{\cdot}5$. This belt is different in character from the Johnston Island shell because it has no measurable effect on the Čerenkov detector even at Geiger-counter rates of 800 counts per 26·9 s. Both belts are greatly modified when the particles meet the South Atlantic anomaly. Figures 110 and 111 represent respectively B–L and R–λ plots for the excess Geiger-counter

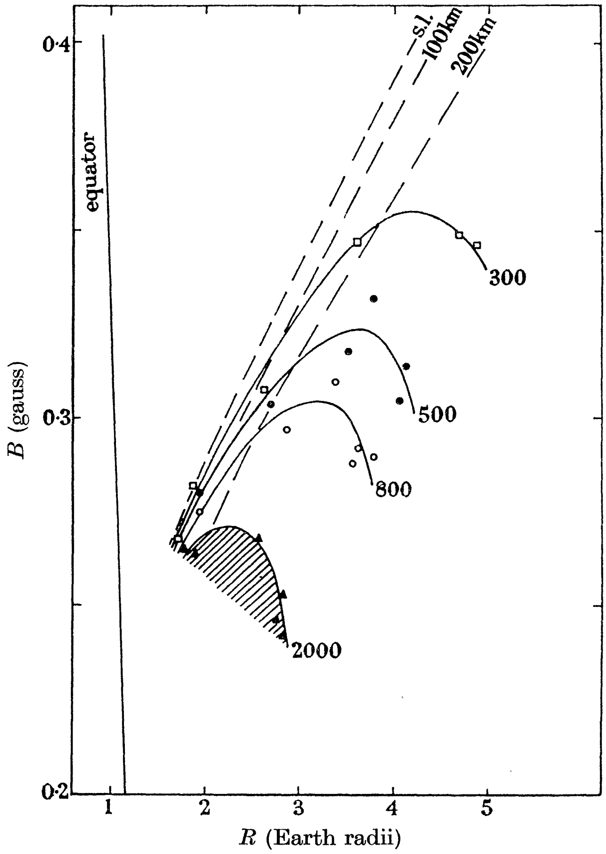

FIGURE 110. B–L plot of the excess of the Geiger-counter rate over the pre-Starfish measurements in the region east of the South Atlantic anomaly and west of Johnston Island. The numbers indicate counts/26·9 s. The dashed lines show the lowest values of B occurring anywhere at sea level, at 100 km and at 200 km altitude on the corresponding L shell.

rates taken to the east of the anomaly where the magnetic shells approach closest to the Earth. Also shown on figures 108 and 110, as a function of the shell value L, is the lowest B value encountered anywhere on the shell at a fixed altitude. Particles observed in the Johnston Island shell have B co-ordinates such that they lie above the sea-level line and therefore they enter the atmosphere near the anomaly. Consequently, no trace of the shell is to be seen in figure 110. Similarly, the contours in the broader belt corresponding to rates of less than 800 counts per 26·9 s lie on magnetic shells which approach within 400 km of the surface. Most of these particles are removed by the anomaly and do not appear in figure 110.

The origin of the particles in the broad belt is obscure. They do not seem to belong to the Johnston Island shell since there is a clear gap at $L = 1{\cdot}5$ between the belts. The absence of any effect on the Čerenkov detector argues against the belt being due to fission fragment electrons and it is unlikely that these particles are from neutron decay. At $L \sim 2{\cdot}5$, Killeen *et al.* (1963) calculate the flux of neutron decay electrons from a fission bomb to be $2 \times 10^5/\text{cm}^2$ close to the Earth.

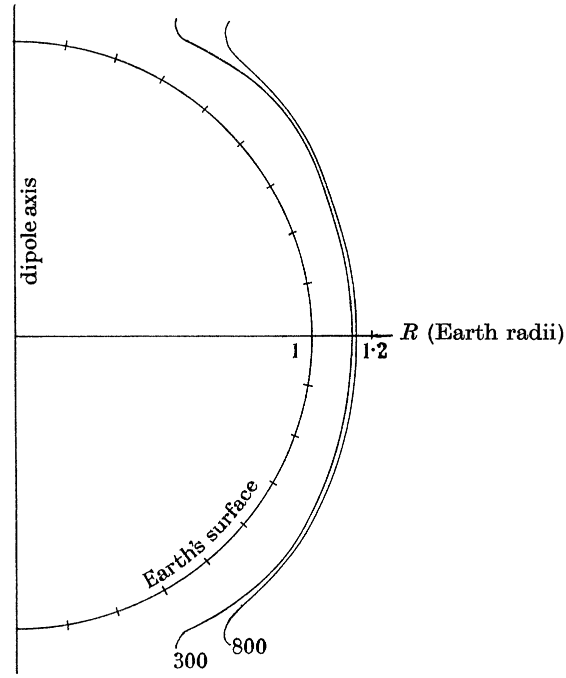

FIGURE 111. R–λ plot of the Geiger-counter intensity contours inferred from figure 6 for a dipole representation of the Earth's field. The position at the Earth's surface represents an average for all longitudes.

If we increase this flux by a factor of 20 to include the possibility of a fusion bomb and take the calculated value of 10^{-6} for the counter efficiency, we obtain a rate of *ca.* 50 per 26·9 s. Rates of up to 800 per 26·9 s were observed in the broad belt in regions where the particle lifetime is about one longitudinal revolution. Since the rate must be higher in the region of particle trapping, the neutron decay source seems to be insufficient, even if we have underestimated the Geiger-counter efficiency by a factor of 10. The ratio of the response of the two detectors is consistent with the particles in this region being outer belt electrons. Possibly some of the outer belt particles, which have had their mirror points redistributed by the hydromagnetic shock wave from the explosion, are still being scattered down into the atmosphere from trapped orbits. This broad belt of enhanced intensity does not persist for much more than a day.

5. The quasi-permanent artificial radiation belt

We shall now discuss the additional particle population existing in trapped orbits and having a long lifetime. Contours of the total flux or Starfish electrons have been published by Van Allen, Frank & O'Brien (1963), Brown & Gabbe (1963), and Hess (1963*b*). During July, Brown & Gabbe report that up to $L = 4$ the energy spectrum of the electrons of around 800 keV was similar to that for fission fragment β-particles but that an excess of particles was observed at lower energies, while Mozer, Elliott, Mihalov, Paulikas, Vampola & Freden (1963) found that in September a fission fragment spectrum was only applicable at $L < 1{\cdot}6$ and at energies of 2 MeV and greater.

Ariel I was situated on the $L = 3$ shell when it first detected radiation directly attributable to the Starfish explosion. Six minutes after the event both detectors saturated (see figure 105, burst B). The saturation of the Čerenkov detector accompanied by a Geiger-counter rate > 30/s has already been ascribed to the presence of fission fragment electrons from observations in the Johnston Island shell, and it is natural to interpret this observation in the same way even though the L value is much higher than that of the shell through the explosion. It seems unlikely that these particles could be outer belt electrons accelerated by the hydromagnetic disturbance, since they appear with a delay of 6 min whilst the largest magnetic fluctuations were seen at ground level within 2 min of the explosion. An alternative explanation is possible in terms of fission fragments which emerge from the explosion electrically neutral and are then able to travel freely through the field for a distance of at least 5500 km to the nearest point which is on both the $L = 3$ shell and the satellite meridian. Here they decay to inject electrons into trapped orbits. The 6 min delay would then correspond to a fission fragment velocity of 15 km/s and therefore to a temperature of *ca.* 10^6 °K on emission from the explosion, which is a reasonable value.

If neutral fission fragments emerged in sufficient quantities there is no need to postulate a rising bubble of plasma containing fission fragments to populate the higher L shell with energetic electrons, and the confinement of the debris to within 700 km altitude implied by the distribution of the Johnston Island shell is satisfied. According to data from Injun I (O'Brien *et al.* 1962*a*) the peak in the flux of trapped electrons lies between $L = 1{\cdot}18$ and $L = 1{\cdot}22$. These shells pass over Johnston Island at between 700 and 1000 km altitude—slightly higher than the shell described here. However, Injun I was measuring radiation with a long lifetime against atmospheric loss processes, while the particles in the Ariel I shell are lost catastrophically in less than one longitudinal revolution and cannot build up in intensity as a result of continuing injection. Thus the shell centred at $L = 1{\cdot}20$ could be caused by injection from a high altitude tail to the distribution of fission fragments; alternatively, multiple Coulomb-scattering upwards of electrons originally injected at 700 km would result in some filling of the $L = 1{\cdot}20$ shell. From Injun I measurements O'Brien and his co-workers find the total number of particles trapped in the field to be *ca.* 10^{24}, which is small compared to the figure of *ca.* 10^{27} for the total number of electrons presumed to be released in the explosion, chiefly at less than 700 km altitude. Again, the observations do not require the propagation of a bubble of debris out to several Earth radii.

Although the peak intensity in the flux of Starfish electrons occurs around $L = 1{\cdot}20$, some additional particles also appear at much higher L values, which we identify as fission fragment β-particles because they produce saturation in the Čerenkov detector. Figure 112 shows the subsatellite points where the Čerenkov detector saturated on 9 and 10 July, the satellite being near perigee on passes moving north-eastward and near apogee on passes moving south-eastward. Saturation at perigee only occurs in the region where particles are lost into the South Atlantic anomaly.

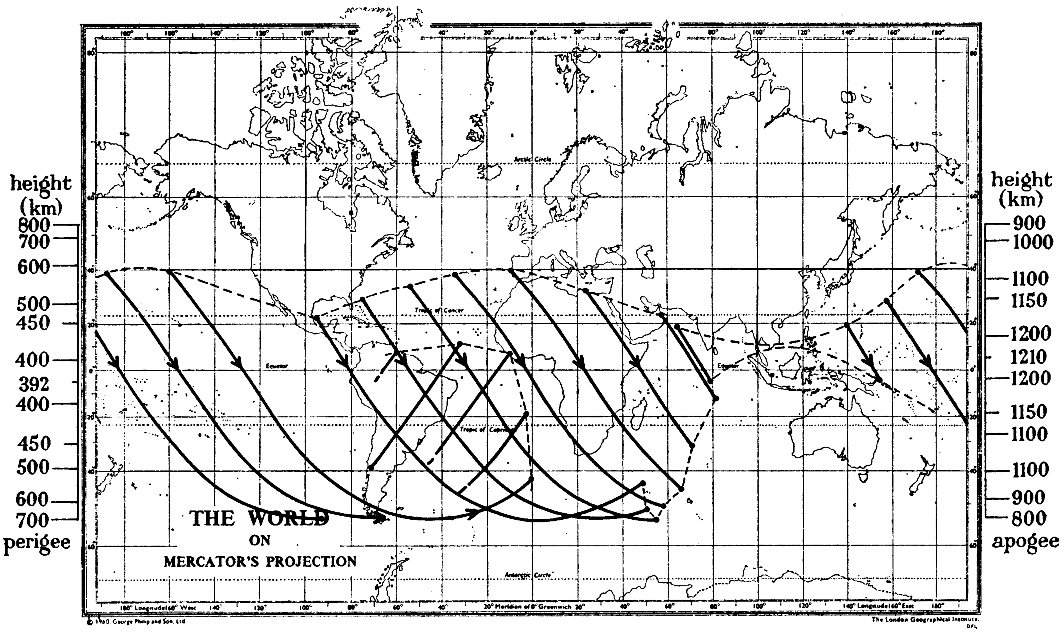

FIGURE 112. Positions of the subsatellite point where the Čerenkov detector saturated on 9 and 10 July, the satellite being near perigee on passes moving north-eastward and near apogee on passes moving south-eastward.

We have already argued that fission fragment electrons are required to saturate the Čerenkov detector and that neutron decay electrons and outer belt electrons cannot have any appreciable effect. Furthermore, acceleration of outer belt particles is unlikely to have taken place. Assuming, therefore, a pure fission fragment spectrum, we tentatively estimate that a total omni-directional flux at all energies of $5 \times 10^6\ \mathrm{cm^{-2}\ s^{-1}}$ is required to cause saturation. In figure 113 we have added the contour corresponding to this counting rate to the R–λ diagram prepared by Van Allen *et al.* (1963) and by Hess & Nakada (1962). The Ariel contour extends to $L = 6{\cdot}5$, thus adding to the results obtained by Injun I on 9 July. It will be shown later that the energy spectrum is modified at high L values, but this will not change our basic conclusion that electrons from fission fragments were injected out to at least $L = 6{\cdot}5$. We have at present no data to compare with Hess's diagram for the Telstar data of 16 July.

Any spatial variation in the energy spectrum of the additional trapped radiation results in a corresponding spatial variation in the ratio of the Geiger-to-Čerenkov-detector counting rates. We have therefore investigated the dependence of this ratio on L. As a measure of the ratio, we have used the Geiger-counter rate corresponding to the saturation of the Čerenkov detector, and this rate is plotted against L in figure 114 for the data obtained during the period 9 to 12 July. Solid

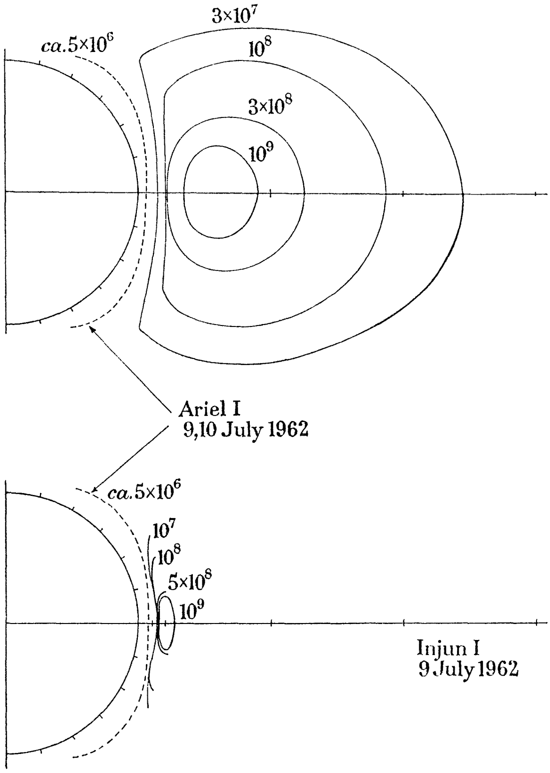

FIGURE 113. Diagrams of the omnidirectional flux of Starfish electrons prepared by Hess & Nakada for 16 July, based mainly on Telstar data, and by O'Brien, Laughlin & Van Allen for 9 July, based on Injun I data. The flux contour deduced from the Ariel I Čerenkov detector is added to both diagrams.

circles correspond to observations at B values such that the trapped particles do not approach closer than 200 km to the surface, while open circles correspond to particles which do approach within 200 km at some longitudes. It will be shown that 200 km represents a suitable limit to the trapping zone. For trapped particles it can be seen that the Geiger-counter rate corresponding to saturation of the Čerenkov counter falls with increasing L value. Observations in the Johnston Island shell, where a fission fragment spectrum is expected, generally give Geiger-counter rates corresponding to Čerenkov saturation which are greater than 1000 per 26·9 s (see, for example, figure 115). Thus at $L < 2$, the Geiger/Čerenkov ratio is consistent with the spectrum obtained from fission fragment electrons, but at higher values the spectrum is different. An increased proportion of low energy electrons from neutron decay, at high L values, cannot explain this result because we know that during the first 6 min after the nuclear explosion the Čerenkov detector showed no measurable response to neutron decay electrons. Indeed, the Geiger-counter rate corresponding to saturation should increase if neutron decay electrons made a significant contribution. The chief contribution to the Čerenkov rate at saturation comes from the 2 to 4 MeV region of the fission spectrum, and we therefore interpret the lower Geiger-counter rate, required for saturation at high L values, as the result of softening of the fission spectrum by the removal of electrons of *ca.* 10 MeV which are counted by the Geiger with high efficiency.

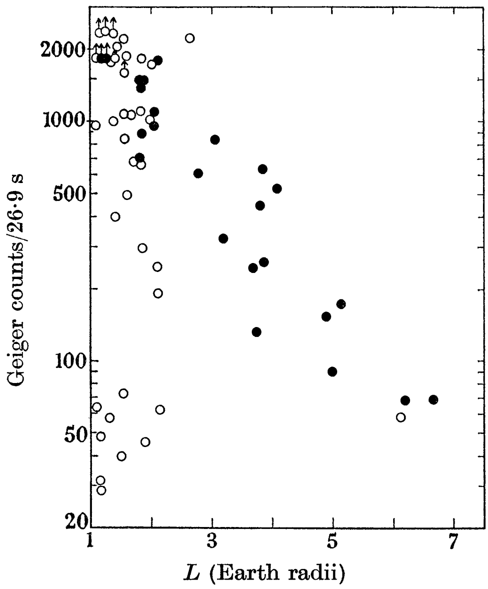

FIGURE 114. The Geiger-counter rate corresponding to the saturation of the Čerenkov detector plotted against L value data obtained from 9 to 12 July. Solid circles correspond to particles which do not approach closer than 200 km from the Earth, and open circles to particles which approach within 200 km.

The more energetic electrons trapped at high L values may be removed from the trapping region by interaction with hydromagnetic waves. The greatest change in the pitch angle occurs when the particle is in gyro-resonance with the wave (see, for example, Dungey 1963). The resonance condition for particles moving much faster than the wave is given by

$$(n_A v \cos\theta)/V_A = n_c,$$

where V_A and n_A are respectively the wave velocity and frequency, v and n_c are respectively the particle velocity and cyclotron frequency in the magnetic field, and θ is the pitch angle of the particle. For relativistic electrons the cyclotron frequency is given by

$$n_c = 2{\cdot}8H/(1+\epsilon)\ \text{Mc/s},$$

where H is the field strength in Gauss and ϵ is the kinetic energy measured in units of rest energy. Since the power spectrum of hydromagnetic waves in the exosphere is believed to fall off rapidly above a frequency of 1 c/s, and since the particle resonance frequency decreases with increasing energy, we get a lower limit to the energy of a particle which is likely to satisfy the resonance condition by solving the above two equations for ϵ and putting $n_A = 1$ c/s. At $L = 4$ this limit is 7 MeV for an electron moving with a pitch angle of 0° in the equatorial plane. The value for V_A which has been used is that calculated by Parker (1961). It is plausible to suppose, therefore, that the observed softening of the fission spectrum at high L values is due to the loss of the more energetic electrons by this process.

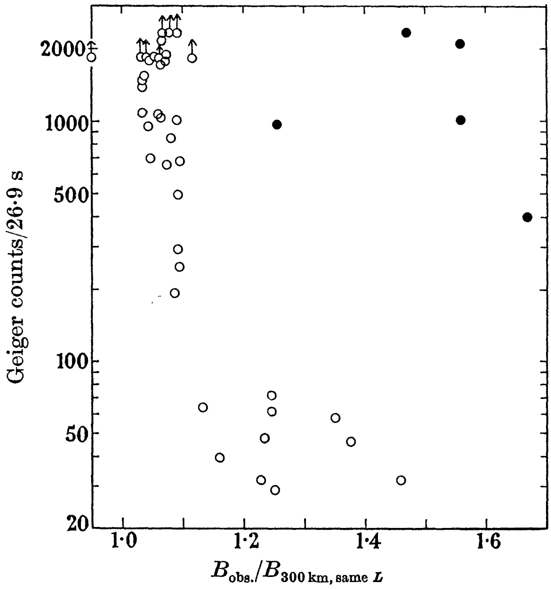

FIGURE 115. The Geiger-counter rate corresponding to the saturation of the Čerenkov detector plotted against the ratio of B at the point of observation to the lowest value of B occurring anywhere at an altitude of 300 km on the same magnetic shell. Solid circles correspond to observations in the Johnston Island shell, open circles to all other observations with $L = 1$ to 2·5, obtained from 9 to 12 July.

Returning to figure 114, and looking now at particles whose trajectories at some points lie below the 200 km limit, we see that they produce a range of Geiger-counter rates corresponding to Čerenkov saturation which all lie below the curve for trapped particles. Without detailed calculation, interpretation of the energy spectrum of these particles is difficult, but it is clear that interaction with the atmosphere is the basic cause of the observed deviation from the fission spectrum. It seems possible that, here again, the lower Geiger-counter rates represent a softening of the spectrum as a result of energy loss by ionization by these particles in process of scattering into the atmosphere. In these circumstances we would expect a progressive change of spectrum with altitude, and evidence for this is presented in figure 115 where we have plotted the Geiger-counter rate corresponding to Čerenkov saturation against the ratio of B at the point of observation to the lowest value of B occurring anywhere at an altitude of 300 km on the same magnetic shell. Thus particles moving on shells with values of this ratio greater than unity approach within 300 km of the surface at some stage in their orbit, and the magnitude of the ratio is a measure of the closeness of their approach. All data in the range $L = 1$ to 2·5 from 9 to 12 July are used. Solid circles were taken in the Johnston Island shell where the continuous injection provides a special case. The other points lie on a curve which depends very steeply on the ratio $B_{obs.}/B_{300\,km}$ around the value 1·1. Below 1·1 the Geiger-counter rates are consistent with a fission fragment spectrum and we therefore take this value of the ratio, corresponding to an altitude of *ca.* 200 km, as the limit of trapping for Starfish electrons at low L.

6. Conclusion

The conclusions arising from these results may be summarized as follows:

(*a*) The hydromagnetic shock wave initiated by the explosion produced a change in the pitch angle distribution of outer belt electrons and resulted in the dumping of some of these particles into the atmosphere within 20 s of the explosion.

(*b*) A shell of electrons centred at $L = 1{\cdot}12$ was formed and maintained for more than a day by the decay fission fragments remaining in the vicinity of Johnston Island. The electrons on this shell disappeared into the atmosphere over the South American geomagnetic anomaly before completing one circuit of the Earth.

(*c*) Most of the fission fragment β-decay electrons were injected into the Earth's magnetic field on L-shells with heights not exceeding 1000 km above Johnston Island, thus implying the confinement of most of the explosion debris to altitudes less than this.

(*d*) Some additional electrons reached L values as high as 6·5 and were probably the result of the decay of neutral fission fragments which moved through the field with velocities corresponding to a temperature of *ca.* 10^6 °K.

(*e*) The energy spectrum of the additional electrons at high L values differed from that for fission β-particles probably because of loss of the highest energy particles through interactions with hydromagnetic waves. The energy spectrum of electrons on L shells below the minimum required for trapping also differed from the fission spectrum. In this case the difference appears to have arisen through ionization loss in the atmosphere.

The conclusions presented in this interim account do not exhaust all the information obtained by Ariel I and further work may bring about some modifications in interpretation. Data on the decay of the artificial belt are scanty but will be published when available.

We wish to thank Dr J. W. Dungey for many helpful suggestions made during the preparation of this paper. We are indebted to the N.A.S.A. for making this joint U.S./U.K. project possible, and to all those members of the N.A.S.A. team who were concerned in the preparation and launching of Ariel I. We wish particularly to thank the two Project Managers, Mr R. C. Baumann and Mr M. O. Robins. Miss W. Lloyd has been largely responsible for the computer programming, and we are particularly indebted to Mrs M. Jackson and her staff at U.K.A.E.A. Risley for their generous assistance in the data processing.

References (Durney, Elliot, Hynds & Quenby)

Brown, W. L. & Gabbe, J. D. 1963 *J. Geophys. Res.* **68**, 607.

Dungey, J. W. 1963 *J. Fl. Mech.* **15**, 74.

Durney, A. C., Elliot, H., Hynds, R. J. & Quenby, J. J. 1962 *Nature, Lond.* **195**, 1245.

Durney, A. C., Elliot, H., Hynds, R. J. & Quenby, J. J. 1964 *Proc. Roy. Soc.* A (preceding paper).

Edwards, P. J., Fenton, A. G., Fenton, K. B. & Greenhill, J. G. 1962 *Nature, Lond.* **196**, 367.

Elliot, H., Quenby, J. J., Mayne, D. W. & Durney, A. C. 1961 *J. Brit. Instn Radio Engrs*, **22**, 251.

Gardner, C. S., Goertzel, H., Grad, H., Morawetz, C. S., Rose, M. H. & Rubis, H. 1958 *Proc. Second U.N. Int. Conf. on Peaceful Uses of Atomic Energy*, **31**, 15/P/374.

Gill, P. J. 1962 *New Zealand J. Geology Geophys.* **5**, 943.

Gregory, J. B. 1962 *Nature, Lond.* **196**, 508.

Hess, W. N. (ed.) 1963*a* Collected papers on the artificial radiation belt from the July 9, 1962 nuclear detonation. *J. Geophys. Res.* **68**, 605.

Hess, W. N. 1963*b* *J. Geophys. Res.* **68**, 667.

Hess, W. N. & Nakada, P. 1962 *Science*, **138** (3536), 53–54.

Killeen, J., Hess, W. N. & Lingenfelter, R. E. 1963 *J. Geophys. Res.* **68**, 4637.

Latter, R., Herbst, R. F. & Watson, K. M. 1961 *Ann. Rev. Nucl. Sci.* **11**, 371.

McIlwain, C. E. 1961 *J. Geophys. Res.* **66**, 3681.

Mozer, F. S., Elliott, D. D., Mihalov, J. D., Paulikas, G. A., Vampola, A. L. & Freden, S. C. 1963 *J. Geophys. Res.* **68**, 641.

Nuclear explosions and their effects 1956 Publications Division, Ministry of Information and Broadcasting, Government of India (p. 95).

O'Brien, B. J., Laughlin, C. D. & Van Allen, J. A. 1962*a* *Nature, Lond.* **195**, 939.

O'Brien, B. J., Van Allen, J. A., Laughlin, C. D. & Frank, L. A. 1962*b* *J. Geophys. Res.* **67**, 397.

Parker, E. N. 1961 *J. Geophys. Res.* **66**, 693.

Pieper, G. F. 1963 *J. Geophys. Res.* **68**, 651.

Van Allen, J. A., McIlwain, C. E. & Ludwig, G. H. 1959 *J. Geophys. Res.* **64**, 271.

Van Allen, J. A., Frank, L. A. & O'Brien, B. J. 1963 *J. Geophys. Res.* **68**, 619.